

FORMATION OF CYCLOIDAL DUST DEVIL TRACKS BY REDEPOSITION OF COARSE SANDS IN SOUTHERN PERU: IMPLICATIONS FOR MARS.

D. Reiss¹, M. I. Zimmerman^{2,3} and D. C. Lewellen⁴,
¹Institut für Planetologie, Westfälische Wilhelms-Universität, Münster, Germany (dennis.reiss@uni-muenster.de),
²NASA/Goddard Space Flight Center, Greenbelt, MD, USA, ³NASA Lunar Science Institute, NASA Ames Research Center, Moffett Field, CA, USA, ⁴West Virginia University, Morgantown, WV, USA.

Background: On Earth, dust devil tracks (hereinafter DDTs) are rarely observed in satellite imagery [1-4] and in situ studies were so far only performed in China [3;5]. First in situ investigations of DDTs on Earth showed that passages of active dust devils remove a thin layer of fine grained material ($< \sim 63 \mu\text{m}$), cleaning the upper surface of coarse sands (0.5 – 1 mm) [3]. This erosional process changes the photometric properties of the upper surface causing the albedo differences within the track to the surroundings [3]. This process is consistent with the formation mechanism proposed by [6] for DDTs on Mars. [4] reported about long- and short lived DDTs in southern Peru. They show a different morphology than usual continuous, low albedo DDTs on Earth and Mars. They have a low albedo cycloidal pattern which is in some areas accompanied by bright margins [4]. Low albedo cycloidal DDTs accompanied by bright lateral areas are still visible after 5 years (long-lived), whereas DDTs without bright lateral areas disappear in less than six months (short-lived) [4]. Based on satellite imagery, their formation was suggested to be due to exposed coarse surface materials (dark cycloidal central track) and fallout of sand-sized material along the edges (bright margins) [4], whereas the formation of shorter-lived DDTs was ascribed to erosion of dust exposing coarser sand sized material [4] equivalent to the previously described formation mechanism [3,6]. Based on our in situ investigations of the DDTs in southern Peru we will show that these proposed formation mechanisms for the Peruvian DDTs and the hypothesis for the longevity of DDTs [4] are not valid. Long- and short-lived DDTs were analyzed in southern Peru in two different study areas: 1) Southwest of the city of Ica at 14.45°S and 75.84°W (long-lived DDTs), and 2) West of the city of Ica at 14.19°S and 75.88°W (short-lived DDTs).

Long-lived DDTs: Based on satellite imagery more than 20 well defined DDTs can be observed in study area 1. Multitemporal images (from 2003, 2005 and 2010) together with our field survey in 2012 reveals that DDTs remain visible for more than 9 years. In plan view the DDT is characterized by a low albedo cycloidal pattern which is accompanied by bright lateral areas (Fig. 1A-C). The alluvial fan surface where the long-lived DDTs are found can be classified as a desert pavement. Grain size analysis shows that the upper surface layer is dominated by very coarse sand grains (1 – 2 mm). Aeolian landforms such as ripples cannot be found indicating a stable surface with no or low aeolian transport processes. This is in agreement with the angular to subangular grain shape of the very coarse sands resting on top of a fine grained substrate composed of clay, silt and fine sand ($< 0.25 \text{ mm}$). Fig. 1D-F shows example surface areas from the low albedo DDT, from the high albedo lateral area of the DDT, and from the undisturbed desert pavement outside the DDT, respectively. The low albedo surface area inside the DDT exhibits a higher abundance of very coarse sands compared to the nearby desert pavement. In contrast, the high albedo lateral area of the DDT shows a very low abundance of very coarse sands compared to the low albedo DDT area as well as to the undisturbed desert pavement outside the DDT area. This implies that very coarse sand material from the desert

pavement was eroded by the outer regions of the vortex of a passing dust devil and deposited within the dust devil center. The long lifetime of the DDTs can be explained by their occurrence on aeolian inactive desert pavements. Field experiments on desert pavements showed that the recovery of areas cleared from stones and granules happens at a rate of about 1 % per year on a 40 cm² plat, thus implying a full recovery within 80 years [7].

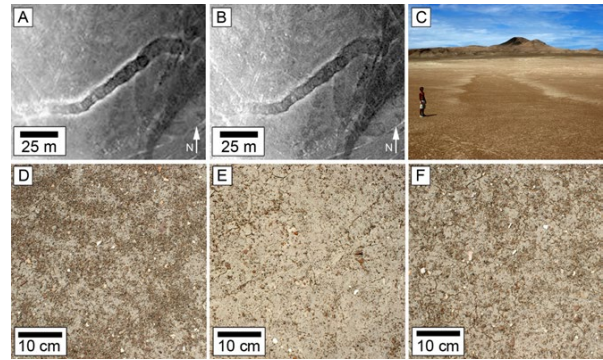


Figure 1. Long-lived DDTs in study area 1. (A-C) Chronological sequence of high resolution satellite images and field survey (A) DDT is first visible on 14 November 2005 (Quickbird 2 satellite image acquired through Bing Maps, $\sim 65 \text{ cm/pxl}$). Note the bright lateral areas along the DDT. (B) DDT on 14 March 2010 (GeoEye-1 satellite image acquired through Google Earth, $\sim 50 \text{ cm/pxl}$). Note the cycloidal pattern of the dark track area. (C): Field photo of DDT in southwest direction on 9 February 2012. (D-F) Surface properties: (D) Area within the dark track area. (E) Area within the bright margin of the dark track. (F) Undisturbed desert pavement area.

Short-lived DDTs: In study area 2, DDTs are abundant in high-resolution satellite images (Fig. 2A). In contrast to study area 1, multi-temporal satellite imagery reveals that their lifetime is less than about one year. Similar to the described long-lived DDTs they show a low albedo cycloidal pattern, but in most cases no bright lateral areas. During our field work several dust devils were observed, some of them leaving tracks (Fig. 2B). The study area consists of a sand sheet characterized by coarse-grained ripples $\sim 3 \text{ cm}$ high and with a wavelength of $\sim 75 \text{ cm}$. Grain size analyses show that the ripples are dominated by coarse to very coarse sand (0.5–2 mm). Within the ripple troughs bright patches of underlying fine grained substrate composed of clay, silt and fine sand ($< 0.25 \text{ mm}$) are exposed (Fig. 2C). Detailed views of the surfaces outside and within the DDT (Fig. 2C and D) shows that the bright patches are covered by coarse sands; hence exhibiting a lower albedo. This implies that the formation of these short-lived DDTs is caused by the redeposition of coarse sands from the outer regions of the vortex towards the dust devil center as it is the case in study area 1. The lack of bright lateral areas can be explained by the much larger amounts of coarse sand grains of the sand sheet compared to the desert pavement in study area 1. The shorter lifetime of DDTs can be explained by their occurrence on an active aeolian sand sheet leading to obliteration when the ripples within the low albedo zone are reorganized and bright patches reoccur.

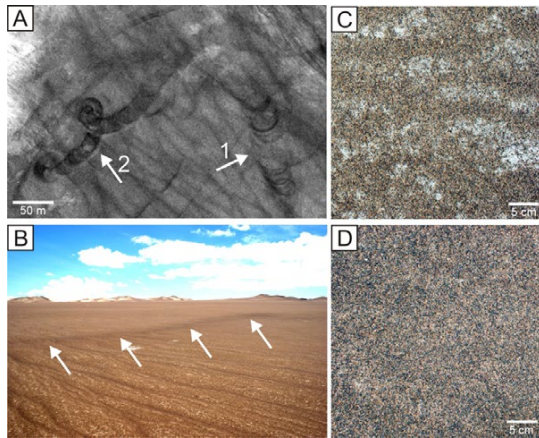


Figure 2. Short-lived DDTs in study area 2. (A) High res. satellite image (accessed through Google Earth) of cycloidal DDTs in study area 2. Note the similar morphologies of DDT 1 (white arrow) to the martian DDT in Fig. 4C and of DDT 2 (white arrow) to the martian DDT in Figure 4D. (B) Observed and analyzed DDT (white arrows). (C) Detailed view of an undisturbed ripple trough outside the DDT. (D) Detailed view of a ripple trough inside the DDT.

Model results: As part of a longstanding effort to understand tornado structure, intensification, and debris dynamics [8,9 and references therein] over 60 large-eddy simulations have been performed varying tornado intensity, corner flow structure, and sand-like debris type. These simulations directly apply to dust devils: like tornadoes they include a near-surface inflow that turns rapidly upward in the corner flow, characteristic velocity and radial scales aloft, surface-relative translation, and formation of surface marks. The simulation code includes sophisticated treatments of surface friction and debris pickup/deposition [18,19], and it records debris removal and deposition to produce surface marks.

The Peruvian scenarios investigated in the present work provide an ideal comparison with the simulations, since the available debris is nearly monodisperse. Assuming a velocity scale $V_c = 10 \text{ m s}^{-1}$ [10], radial scale $R_c = 10 \text{ m}$ (from the observed Peruvian tracks), and a surface roughness length $z_0 \sim 1 \text{ mm}$ [11], a subset of the tornado simulations are directly scalable (by a factor of 10 in velocity and space, with simulated tornado velocities $V_c \sim 100 \text{ m s}^{-1}$, radii $R_c \sim 100 \text{ m}$, and surface roughness lengths $z_0 \sim 1 \text{ cm}$). Two sample tracks are shown in Fig. 3, which are taken from simulations with a high ratio of swirl to flowthrough, $S_c = 9.3$ [9], moderate intensity, $A_a = V_c^2 / (gR_c) = 2.2$ [8], translation speed $A_t = U/V_c = 0.15$, and two different types of debris, $A_v = V_c/w_t = 22.7$ and $A_v = 6.8$, where g is gravity, U is translation speed in m s^{-1} , and w_t is debris terminal speed in freefall, in m s^{-1} [8]. The dust devil scales assumed, with $U \sim 2 \text{ m s}^{-1}$, give comparable estimates of $A_a \sim 1$ and $A_t \sim 0.2$; assuming a debris radius 1-2 mm and mass density 500 kg m^{-3} gives $w_t \sim 2.5$ - 4.7 m s^{-1} and $A_v \sim 2$ -4 for terrestrial dust devils on these scales.

The case of Fig. 3a can be considered to have “lighter debris” and the case of Fig. 3b has “heavier debris”. Both cases have a lateral area of removal (red signatures) around a central cycloidal track of deposition (blue signatures) dropped underneath the corner flow [12]. Lateral asymmetry in the removal is produced by moderate vortex translation [8]. In Fig. 3a there is also intermittent deposition to the right of the vortex from the debris cloud aloft [cf. 12]. Fig. 3b is most readily comparable to the Peruvian dust devils, given our assumptions about the wind field scalings, swirl ratio, and choice of debris parameter A_v . Since track albedo in the field correlates inversely with particle size at the surface, we suggest that the track of Fig. 3b would

produce dark cycloids surrounded by a brighter region (due to exposed desert pavement), consistent with the field observations described herein.

Laboratory studies: Our DDT formation hypothesis is also consistent with laboratory work of [13]. The laboratory dust devils (eroded sand material (0.2 mm) from a zone which was 1 to 4 times the diameter of the vortex [13]. The unique cycloidal DDTs were formed by deposition of the eroded sand material in an annular pattern within the dust devil center [13].

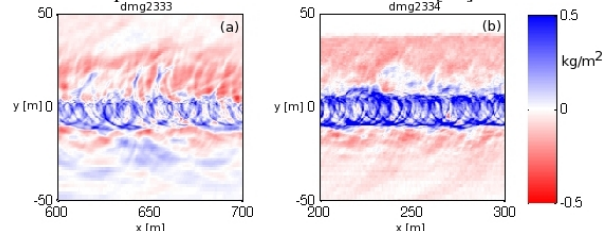


Figure 3. Simulated net deposition by a dust devil vortex with high swirl ratio $S_c = 9.3$, moderate intensity $A_a = 2.2$, translation parameter $A_t = 0.15$, and debris type (a) $A_v = 22.7$ (1 mm diameter / mass density 666 kg m^{-3}) and (b) $A_v = 6.8$ (1 mm / 5200 kg m^{-3}). The vortex has moved from left to right across the surface (toward $+x$). The y -coordinate is measured with respect to the vortex center far aloft. Max dep./rem. corresponds to \sim one monolayer of 1 mm debris.

Implications for Mars: Most DDTs on Mars are characterized by continuous low albedo tracks (Fig. 4 A and B) and do not show the distinctive cycloidal pattern observed in southern Peru. In situ analyses of this type of DDTs by the MER Spirit implies a formation due to dust removal exposing darker coarse grained sands [6], a formation process which was also observed on Earth [3]. However, several DDTs on Mars show a low albedo cycloidal pattern (Fig. 4 C and D) which indicates - based on our field observations and model results - that they are formed by redeposition of sand-sized material instead of dust removal.

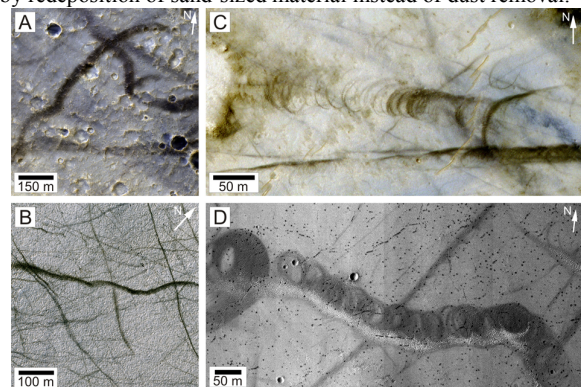


Figure 4. Examples of different martian DDT patterns. (A) Continuous low albedo DDTs in Gusev crater (PSP 006524 1650). (B) Continuous low albedo DDTs (ESP_013751_1115). (C) Cycloidal DDT, note the similarity to the terrestrial DDT 1 in Fig. 2A (PSP_006477_1745). (D) Cycloidal DDT, note the similarity to the terrestrial DDT 2 in Fig. 2A and the bright lateral area on the southern edge of the dark track (HiRISE image PSP_005910_1745).

References: [1] Rossi A.P. and Marinangeli L. (2004) GRL, 31, L06702. [2] Neakrase L.D.V. et al. (2008) GSA, 40, abstract #262. [3] Reiss D. et al. (2010) GRL, 37, L14203. [4] Hesse, R. (2012) Aeolian Res., 5, 101-106. [5] Reiss et al. (2011) Icarus, 211, 917-920. [6] Greeley R. et al. (2005) JGR, 110, E06002. [7] Haff P.K. and Werner B.T. (1996) Quat. Res., 45, 38-46. [8] Lewellen D.C. et al. (2008) JAS, 65, 3247-3262. [9] Lewellen W.S. et al. (1997) JAS, 54, 581-605. [10] Farrell et al. (2004) J. Geophys. Res. 109. [11] Blumberg and Greeley (1992) J. Arid Env. 25, 39-48. [12] Lewellen and Zimmerman (2008) Proc. AMS Sev. Loc. Storms Conf. [13] Greeley R. et al. (2004) GRL, 31, L24702.